AMERICAN SOCIETY FOR MICROBIOLOGY | Molecular and Cellular Biology®

RESEARCH ARTICLE

The Conserved CNOT1 Interaction Motif of Tristetraprolin Regulates ARE-mRNA Decay Independently of the p38 MAPK-MK2 Kinase Pathway

Alberto Carreño,[a] **Jens Lykke-Andersen**[a]

[a]Department of Molecular Biology, School of Biological Sciences, University of California San Diego, La Jolla, California, USA

ABSTRACT The regulation of the mRNA decay activator Tristetraprolin (TTP) by the p38 mitogen-activated protein kinase (MAPK) pathway during the mammalian inflammatory response represents a paradigm for the control of mRNA turnover by signaling. TTP activity is regulated through multiple phosphorylation sites, including an evolutionary conserved serine in its CNOT1 Interacting Motif (CIM) whose phosphorylation disrupts an interaction with CNOT1 of the CCR4-NOT deadenylase complex. Here we present evidence that the TTP CIM recruits the CCR4-NOT deadenylase complex and activates mRNA degradation cooperatively with the conserved tryptophan residues of TTP, previously identified to interact with CNOT9. Surprisingly, the TTP CIM remains unphosphorylated and capable of promoting association with the CCR4-NOT complex and mRNA decay upon activation of p38-MAPK-activated kinase MK2, a well-established regulator of TTP activity. The CIM is instead targeted by other kinases including PKCα. These observations suggest that signaling pathways regulate TTP activity in a cooperative manner and that the p38 MAPK-MK2 kinase pathway relies on the activation of additional kinase pathway(s) to fully control TTP function.

KEYWORDS Tristetraprolin, mRNA degradation, mRNA stability, posttranscriptional RNA-binding proteins, protein phosphorylation

mRNA turnover is a critical step in the regulation of gene expression and improper regulation of mRNA stability can promote the development of pathologies including neurodegenerative disorders, cancer, and chronic inflammation (1). mRNA degradation occurs by a multistep process that generally initiates with the removal of the poly(A)-tail, followed by decapping of the 5′ 7-methylguanosine cap, and exonucleolytic decay from either the mRNA 3′ or 5′ end (1, 2). Transcriptome-wide analyses have revealed considerable differences in stability between mRNAs with half-lives in mammals ranging from minutes to hours or days (3, 4). Factors that affect the stability of mRNAs include sequences found within the 3′ or 5′ untranslated regions (UTRs), and the codon usage within the open reading frame (1–3, 5). Importantly, there are transcripts whose stability change in accordance with signaling events in the cell. These transcripts are often regulated by RNA-binding proteins, which are themselves targets of post-translational modification. The general principles by which these post-translational modifications affect the activation of mRNA decay remain poorly defined.

The RNA binding protein Tristetraprolin (TTP; also known as ZFP36 or TIS11) is an mRNA destabilizing factor that recruits factors promoting translation repression, deadenylation, decapping, and exonucleolytic decay (6–9). TTP is a highly regulated protein whose post-translational modifications have been shown to affect its stability, localization, and decay activity (10–13). TTP is best known for its role in resolving the inflammatory response by promoting the degradation of pro-inflammatory cytokine mRNAs

Address correspondence to Jens Lykke-Andersen, jlykkeandersen@ucsd.edu.

The authors declare no conflict of interest.

Received 15 February 2022
Returned for modification 7 March 2022
Accepted 8 July 2022
Published 3 August 2022

that contain adenosine-uridine rich elements (AREs) in their 3′ UTRs (14–18). Structurally, TTP consists of a zinc-finger domain responsible for RNA binding, flanked by amino- (N-) and carboxy- (C-) terminal domains, each of which are capable of promoting mRNA decay (6). Two vertebrate paralogs of TTP, BRF1 (also known as ZFP36L1 and TIS11b) and BRF2 (also known as ZFP36L2 and TIS11d), which also mediate degradation of ARE-containing transcripts, contain zinc finger domains that are highly similar to that of TTP, but N- and C-terminal domains that are distinct, except for a highly conserved region at the extreme C-terminus (10, 19–21).

Recent attention has been turned toward this conserved C-terminal region of the TTP protein family. Studies examining the structural basis of TTP's association with the central cytoplasmic deadenylase, the CCR4-NOT complex, revealed an interaction between the CCR4-NOT scaffold protein, CNOT1, and this C-terminal region of TTP, which was therefore named the CNOT1-Interacting Motif (CIM) (8, 22). Supporting the importance of the CIM, deletion of the TTP CIM led to a stabilization of target transcripts (8, 23). The loss of the CIM, however, did not completely ablate the ability of TTP to promote mRNA decay, an observation that was further supported by the development of mice lacking the TTP-CIM, which exhibited an inflammatory phenotype significantly milder than that observed upon the complete loss of TTP (23). Separately, it was demonstrated that TTP has a second interaction with the CCR4-NOT complex via several conserved tryptophan residues that interact with the CNOT9 subunit (9). Mutation of those residues were also shown to stabilize TTP target transcripts. Furthermore, TTP is known to interact with the 4EHP-GYF2 translation repression complex and with decapping factors (6, 7, 24). However, the importance of these interactions for TTP's ability to activate mRNA decay in concert with the CCR4-NOT deadenylase complex remains less well understood.

TTP is a highly post-translationally regulated protein that has been shown to be a target of several kinase pathways. The most well-characterized of these is the p38 MAPK pathway, which is activated during the inflammatory response (25). A downstream kinase in the p38 MAPK pathway, MAPK-activated protein kinase 2 (MK2), targets TTP serine residues 52 and 178 (mouse numbering) whose phosphorylation leads to the stabilization of TTP target transcripts by inhibiting the recruitment of deadenylases (13, 26–28). Furthermore, MK2-mediated phosphorylation of TTP promotes the recruitment of 14-3-3 adaptor proteins, which have been speculated to inhibit degradation factor association, and affect both TTP localization and protein stability (10–12).

Another serine of TTP that undergoes phosphorylation is serine 316 (mouse numbering), an evolutionary conserved serine of the CIM motif. Phosphorylation of this residue has been shown to inhibit association of TTP-family proteins with CNOT1, suggesting that the association of the major deadenylase complex is repressed by phosphorylation (8, 29, 30). However, a separate study using phosphomimetic mutations, suggested that phosphorylation of the CIM of the TTP homolog BRF1 promotes its association with decapping factors and accelerates mRNA decay (30). Although several studies have identified the CIM as a target of MK2 (10, 29, 31), others have implicated the kinases RSK1 and PKA (29, 30). Thus, the importance of the highly conserved CIM and its phosphorylation in TTP regulation and function remains poorly defined.

In this study, to better understand the significance of TTP co-factor interactions in promoting activation of mRNA decay and how these are regulated by phosphorylation, we monitored the combinatorial effects of phosphorylation site and co-factor interaction motif disruptions on TTP function. We find that the CIM acts cooperatively with the conserved tryptophans of TTP to recruit the CCR4-NOT complex and activate mRNA decay, but upon mutation of these motifs, TTP remains unimpaired in its interaction with decapping factors and partially active. Using a phospho-specific antibody, we find that phosphorylation of the TTP CIM occurs with kinetics similar to that of the MK2-phosphorylated TTP serine 178 in stimulated mouse fibroblasts and macrophage cell lines and reduces the ability of TTP to promote mRNA decay. Surprisingly, in the presence of active MK2 kinase the CIM remains unphosphorylated and TTP stays active primarily due to the activity of the CIM. These observations suggest that the CIM

serves as an MK2-independent regulatory module of TTP and that the full range of TTP regulation requires cooperativity between kinase pathways.

RESULTS

The TTP-CIM cooperates with other regions of TTP to promote mRNA decay. To establish a system for monitoring the interplay between the CIM and its phosphorylation with other known functional regions of TTP (Fig. 1A), we utilized a previously established MS2-tethering pulse-chase mRNA decay assay (32) (Fig. 1B) to first test the sufficiency and necessity of the conserved TTP-CIM motif for TTP-mediated mRNA degradation. A tetracycline-inducible β-globin mRNA containing MS2 coat protein binding sites in the 3′UTR was transiently co-expressed in human HeLa Tet-off cells with the MS2 coat protein fused to GFP and the TTP CIM. GFP served as a marker for transfection efficiency, and to stabilize an otherwise unstable MS2 coat protein. The MS2-GFP-CIM fusion protein promoted target mRNA degradation compared to the control MS2-GFP fusion protein alone (Fig. 1C and D), which was expressed at a similar level (Fig. 1E). An increase in mobility of the target mRNA through the gel was also observed over time in the presence of the MS2-GFP-CIM fusion protein over the MS2-GFP control (Fig. 1C; quantified in Fig. 1F), consistent with the previously described function of the CIM in accelerating deadenylation (8). This conclusion was confirmed by oligo-dT and RNase H treatment to remove the poly-A tail, which resulted in the target mRNAs migrating at the same rate (Fig. 1G). Co-immunoprecipitation (co-IP) assays for the MS2-GFP-CIM fusion protein confirmed CNOT1 association as compared with the control MS2-GFP protein (Fig. 1H). Thus, our MS2-coat protein tethering system recapitulates previously reported activities of the CIM (8), and the TTP-CIM is sufficient to accelerate mRNA deadenylation and decay.

Although the TTP-CIM can promote mRNA decay on its own, other regions of TTP have been implicated in mRNA decay as well. We were therefore interested in understanding the importance of the CIM in promoting mRNA degradation in conjunction with other functional motifs of TTP. We first deleted the CIM from full-length TTP and from the carboxy-terminal domain (CTD) of TTP, each fused to the MS2 coat protein, and tested the effect on mRNA degradation. Consistent with previous reports (6), the target mRNA was rapidly degraded upon tethering of both the TTP-CTD and full-length TTP (Fig. 2A to F). Deletion of the CIM greatly stabilized target transcripts in the context of the CTD (Fig. 2A to C), although it only marginally impaired the activity of full-length TTP (Fig. 2D to F). This difference in the contribution of the CIM to mRNA decay promoted by the TTP-CTD and full-length TTP suggests a redundancy of the CIM with other regions of TTP, particularly outside of the CTD.

The TTP-CIM cooperates with conserved tryptophan residues to promote mRNA deadenylation and decay. TTP was previously reported to interact with another component of the CCR4-NOT complex, CNOT9, through its conserved tryptophan residues (Fig. 1A) (9). We were therefore interested in understanding to what extent the CIM and tryptophan residues cooperate to activate mRNA decay. We generated alanine mutants for all conserved tryptophan residues of TTP and the TTP-CTD with the additional mutation of Proline 257, which was previously shown to also contribute to CNOT9 association (9) (Table 1). We performed tethered pulse-chase mRNA decay assays for these mutants with and without CIM deletion. The tryptophan to alanine (WA) mutation caused no significant reduction in activity in the context of the TTP-CTD with or without CIM deletion (Fig. 2A to C). However, for full-length TTP, further stabilization of the target mRNA was observed when the removal of the CIM was combined with mutations in the tryptophan motifs (Fig. 2D to F). This reduction in activity was accompanied by reduced association of TTP and the TTP CTD with the CCR4-NOT complex upon mutation of CIM and tryptophan motifs, as evidenced by reduced association with CNOT1 and CNOT9 (Fig. 2G and H). These observations demonstrate that the conserved tryptophan motifs and the CIM serve to cooperatively recruit the CCR4-NOT complex and activate mRNA decay, presumably via their previously reported interactions with different subunits of the CCR4-NOT complex.

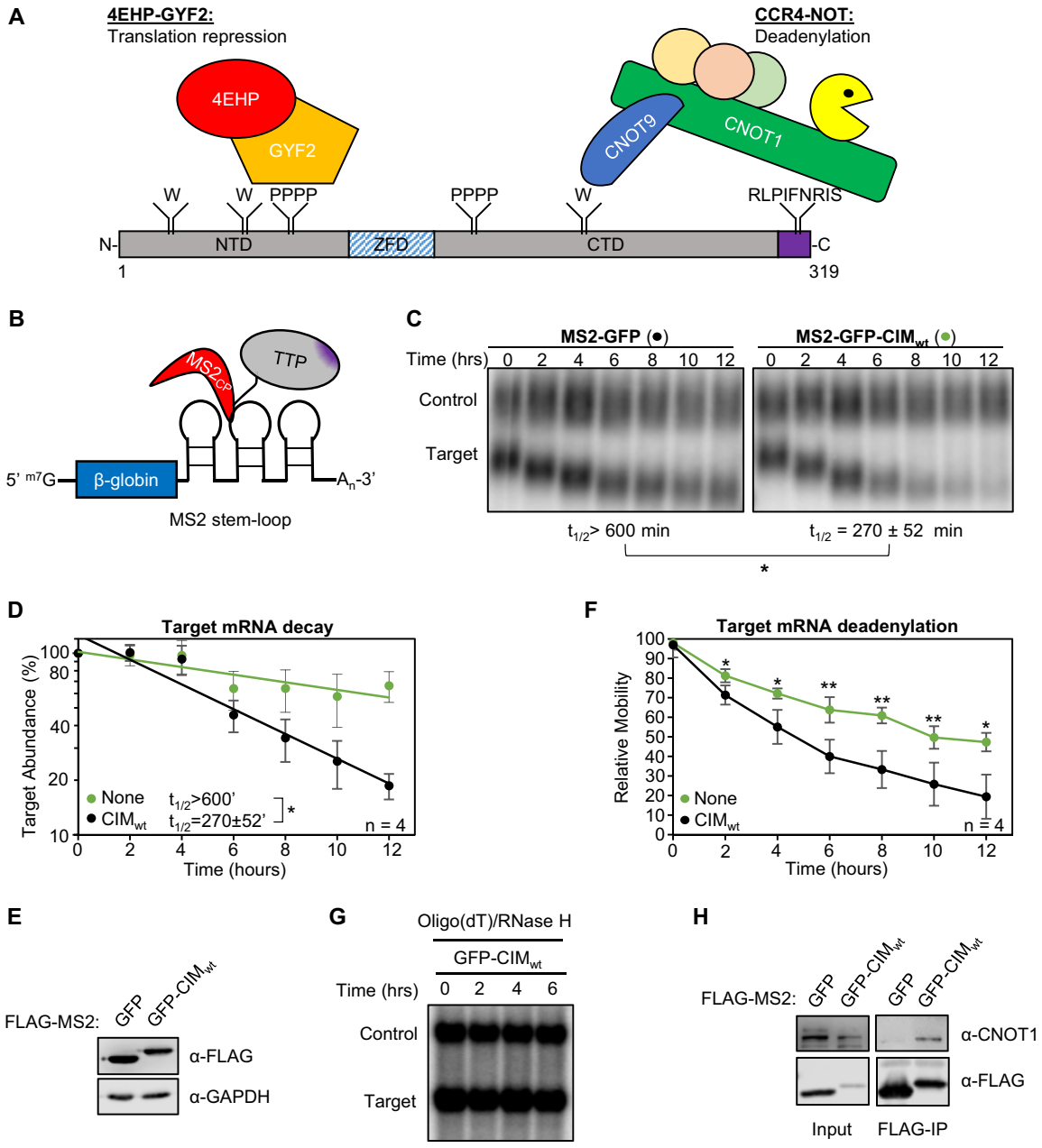

FIG 1 The TTP CIM promotes mRNA deadenylation and decay. (A) Schematic of mouse TTP, highlighting conserved tryptophan residues (W) interacting with CNOT9, tetraproline motifs (PPPP) interacting with the 4EHP-GYF2 translation repression complex, and the CNOT1-interacting motif (CIM), shown in purple. NTD: N-terminal domain, ZFD: Zinc-Finger Domain, CTD: C-terminal domain. (B) Schematic of the tethered mRNA decay assay. A tetracycline-regulated β-globin mRNA containing MS2 coat protein (MS2cp) stem-loop binding sites in the 3'UTR is targeted by MS2-TTP fusion proteins. (C) Representative Northern blots monitoring the degradation in HeLa Tet-off cells over time after transcriptional shutoff by addition of tetracycline, of β-globin mRNA (Target) tethered to MS2-GFP (left) or MS2-GFP-CIM (right) fusion proteins compared to an extended β-globin mRNA (Control) that lacks MS2-coat protein binding sites and is not regulated by tetracycline. The half-life of the target mRNA calculated after normalization to the internal control is shown below each panel with standard deviation from four independent experiments. (D) Graph quantifying mRNA decay assays for β-globin mRNA tethered to MS2-GFP fusion proteins shown in panel C. Dots represent target mRNA abundance relative to the internal control at each time point with standard deviations shown from four independent replicates (n = 4). The curves represent best fits to first-order degradation. Calculated half-lives are given with standard deviation. (E) Western blots monitoring expression levels of indicated FLAG-MS2-GFP fusion proteins in the experiment in panel C. GAPDH serves as an internal control. (F) Graph showing relative band mobilities as a measure of mRNA deadenylation from the experiment in panel C. Dots represent mobility of the target mRNA relative to the control mRNA, with the mobility at time zero set to 100 and the mobility of a deadenylated target mRNA, generated by treatment with oligo-dT and RNase H (panel G), set as 0. Error bars represent standard deviation (n = 4). (G) Northern blot monitoring β-globin mRNA tethered to MS2-GFP-CIM fusion protein in HeLa tet-off cells and treated with oligo-dT and RNase H. (H) Western blots showing proteins co-immunoprecipitating (IP, right panels) with indicated FLAG-MS2-GFP fusion proteins expressed in HEK293T cells. Input samples corresponding to 2.5% of IPs are shown on the left. *, $p < 0.05$, **, $p < 0.01$; student's two-tailed t-test.

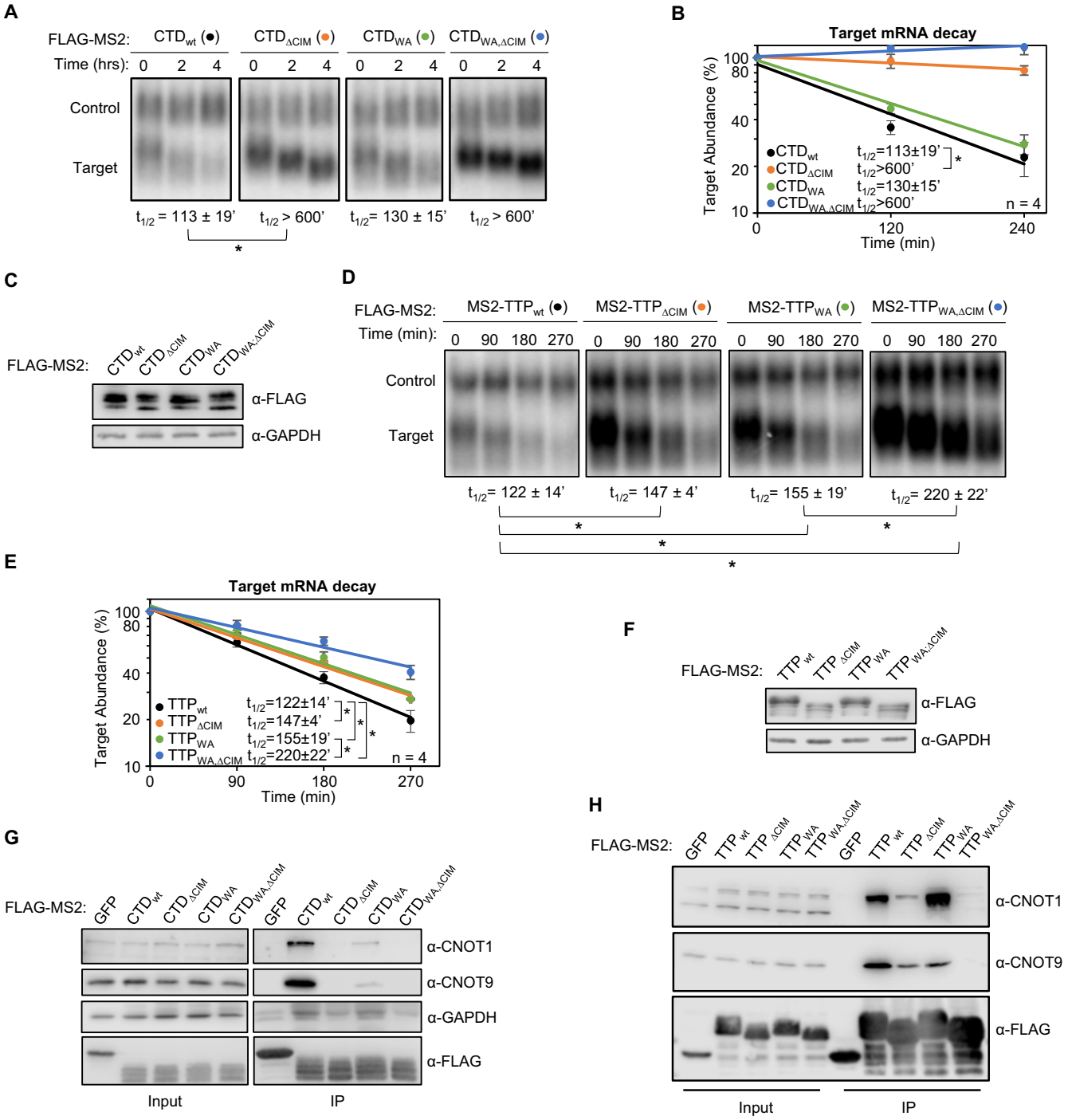

FIG 2 The TTP CIM promotes mRNA decay cooperatively with conserved TTP tryptophans. (A) Representative Northern blots monitoring mRNA decay of β-globin mRNA tethered to TTP-CTD wild-type (wt) or mutant proteins with the CIM deleted (ΔCIM), conserved tryptophans mutated to alanines (WA), or both (WA,ΔCIM). (B) Graph quantifying four repeats of mRNA decay assays in panel A. Error bars represent standard deviation. (C) Western blots monitoring expression levels of TTP-CTD fusion proteins in panel A. (D) Same as panel A, but with wild-type or mutant MS2-TTP full-length fusion proteins. (E) Graph quantifying four repeats of mRNA decay assays in panel D. (F) Western blots monitoring expression levels of TTP fusion proteins in panel D. (G) Western blots showing proteins co-immunoprecipitating (IP, right panels) with the indicated FLAG-tagged MS2-TTP-CTD fusion proteins from HEK293T cells after treatment with RNase A, as compared with input samples (left). IP samples correspond to 2.5% of the input. (H) Same as panel G, but monitoring proteins associated with FLAG-tagged MS2-TTP fusion proteins. *, $p < 0.05$; Student's two-tailed *t*-test.

Mutation of conserved tetraproline motifs does not significantly affect TTP-mediated mRNA decay rates. Other regions of TTP that interact with mRNA repression factors are the tetraproline motifs, which are conserved among TTP orthologs and promote the association with the 4EHP-GYF2 translation repression complex (7, 33).

TABLE 1 TTP mutant proteins

TTP mutant	TTP mutation(s) (mouse numbering)
CTD_{WA}	Δ1-166, W255A, P257A
$CTD_{WA;\Delta CIM}$	Δ1-166, W255A, P257A, Δ304-319
TTP_{WA}	W31A, W61A, W255A, P257A
TTP_{PS}	P64-66S, P191-193S
$TTP_{WA;\Delta CIM}$	W31A, W61A, W255A, P257A, Δ304-319
$TTP_{PS;\Delta CIM}$	P64-66S, P191-193S, Δ304-319
$TTP_{PS;WA;\Delta CIM}$	P64-66S, P191-193S, W31A, W61A, W255A, P257A, Δ304-319
TTP_{S316A}	S316A
TTP_{2A}	S52A, S178A

Mutations in these motifs, and depletion of 4EHP, were previously found to cause increased protein production from TTP target transcripts. Given the interconnected roles of translation repression and mRNA decay, we next performed tethered mRNA decay assays for TTP tetraproline mutants. We found that mutation of TTP tetraproline motifs (PS) did not increase the stability of the tethered target mRNA (Fig. 3A–C). To address whether the tetraproline motifs act cooperatively with the CNOT1 and CNOT9 interaction motifs, we established double and triple mutant TTP proteins. Comparing TTP mutants with and without tetraproline motif mutations revealed no stabilization of the target mRNA attributed to the tetraproline mutations (PS) when combined with the tryptophan mutations (WA) and/or CIM deletion (ΔCIM) (Fig. 3A–G), despite loss of association with CCR4-NOT and GYF2-4EHP complexes as monitored by co-immunoprecitation assays for CNOT1, CNOT9 and GYF2 (Fig. 3H). Interestingly, the TTP triple mutant protein defective in both CCR4-NOT and GYF2-4EHP complex association maintained undisrupted association with DDX6 and EDC4 of the decapping complex (Fig. 3H), suggesting that additional functional motifs exist in TTP that may explain the partial activity of this triple mutant.

TTP is transiently phosphorylated at the conserved CIM serine residue. Having established the degree of cooperativity between the TTP CIM and other known functional motifs of TTP, we next turned to the significance of CIM phosphorylation. We generated and validated a phospho-specific antibody raised against the phosphorylated serine 316 residue of mouse TTP (Fig. 4A). Consistent with a recent report (29), induction of the inflammatory response by serum shock of mouse NIH3T3 fibroblasts (Fig. 4B), or treatment with lipopolysaccharide (LPS) of mouse RAW264.7 macrophages (Fig. 4C), both caused rapid upregulation of TTP accompanied by phosphorylation at TTP serine 316, with kinetics similar to what has been described previously for TTP serine 178 phosphorylation (10, 28).

The TTP-CIM is phosphorylated in a p38 MAPK-MK2-independent manner. The TTP-CIM has been reported as a target of several kinase pathways (10, 29–31), including the p38 MAPK-MK2 pathway, which also targets TTP serines 52 and 178 (10, 28). HeLa cells transiently expressing TTP show detectable levels of phosphorylation of both serines 178 and 316 of TTP (Fig. 5A). Treatment with the p38 MAPK inhibitor SB203580 (34) decreased serine 178 phosphorylation, as expected, whereas serine 316 phosphorylation surprisingly remained unaffected (Fig. 5A). Consistent with this observation, co-expression of TTP or the TTP-CIM in HEK 293 cells with constitutive active MK2 (12, 28) resulted in phosphorylation of TTP serine 178 (Fig. 5B) but not serine 316 (Fig. 5B and C).

Other kinases that have been observed to phosphorylate the CIM of TTP-family proteins include p90 ribosomal S6 kinase 1 (RSK1) and Protein Kinase A (PKA) (29, 30, 35). Another kinase predicted to phosphorylate TTP serine 316 in a kinase prediction algorithm (36) is Protein Kinase C-alpha (PKCα). Treatment of HeLa cells with a PKC inhibitor, Gö6983 (37), decreased TTP serine 316 phosphorylation whereas serine 178 phosphorylation remained unaffected (Fig. 5A). Moreover, constitutive active PKCα increased serine 316 phosphorylation both in the context of full-length TTP (Fig. 5B) and the TTP-CIM (Fig. 5C and D). We also observed an increase in TTP serine 178 phosphorylation in the

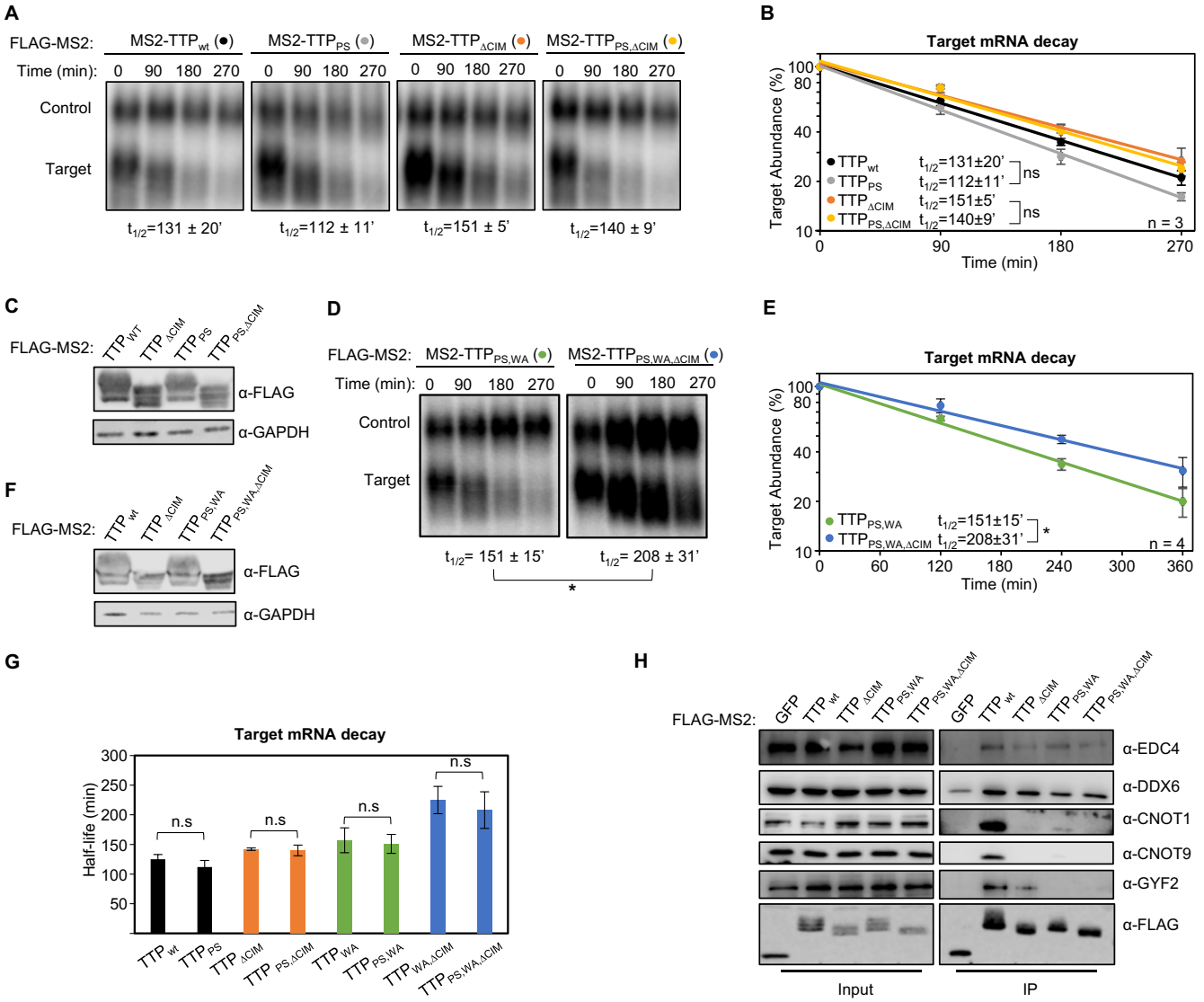

FIG 3 TTP tetraproline motifs do not enhance TTP mRNA decay activity. (A) Representative Northern blots monitoring mRNA decay of β-globin mRNA tethered to indicated MS2-TTP wild-type (wt) or mutant proteins with the tetraproline motifs mutated to serines (PS), the CIM deleted (ΔCIM), or both (PS,ΔCIM). (B) Graph quantifying three repeats of mRNA decay assays in panel A. Error bars represent standard deviation. (C) Western blots monitoring expression levels of TTP fusion proteins in panel A. (D) Same as panel A, with indicated mutant MS2-TTP fusion proteins with tetraproline motifs mutated to serines and conserved tryptophans to alanines (PS,WA), or additional deletion of the CIM (PS,WA,ΔCIM). (E) Graph quantifying four repeats of mRNA decay assays in panel D. (F) Western blots monitoring expression levels of TTP fusion proteins in panel D. (G) Bar-graph comparing half-lives of β-globin mRNA tethered to the indicated MS2-TTP fusion proteins with or without mutation in tetraproline motifs (PS). Error bars represent standard deviation from 3 or 4 experiments. (H) Western blots showing proteins co-immunoprecipitating (IP, right panels) with indicated FLAG-tagged MS2-TTP fusion proteins from HEK293T cells after treatment with RNase A, as compared with input samples (left). IP samples correspond to 2.5% of the input. *, $p < 0.05$; n.s., $p > 0.05$; Student's two-tailed *t*-test.

presence of active PKCα (Fig. 5B), which is likely due to reported activation by PKCα of the p38 MAPK pathway (38). Thus, serine 316 of the CIM can be phosphorylated by kinases including PKCα, but unlike serines 52 and 178, remains unphosphorylated in the presence of active MK2.

MK2-phosphorylated TTP promotes mRNA decay via the CIM. TTP activity has been previously reported to be inhibited by MK2 phosphorylation on serine residues 52 and 178, correlating with decreased association with deadenylation factors as well as the recruitment of 14-3-3 adaptor proteins (10–12, 39). Our observation that the CIM remains unphosphorylated in the presence of MK2 raised the possibility that the CIM continues to promote deadenylation and decay in the presence of active MK2. To test this idea, we performed tethered mRNA decay assays comparing the effect of MK2 on

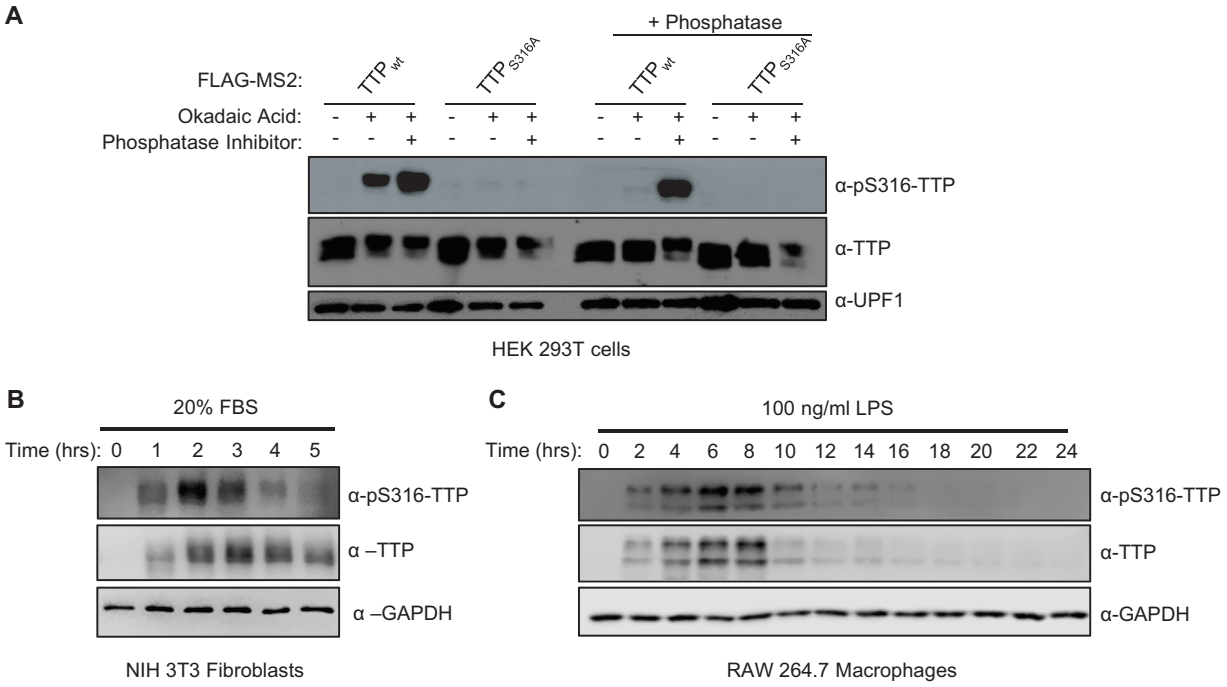

FIG 4 TTP serine 316 is phosphorylated during TTP induction. (A) Western blot validating the anti-pS316-TTP antibody of indicated FLAG-MS2-TTP fusion proteins expressed in HEK293T cells incubated with or without okadaic acid (OA) and treated following cell lysis without (left panels) or with (+ phosphatase, right panels) calf-alkaline phosphatase in the presence or absence of phosphatase inhibitor (PhosphataseArrest I), prior to Western blotting using the anti-pS316-TTP antibody as compared with TTP and UPF1 controls. (B) Western blots monitoring levels of TTP and its phosphorylation at serine 316 (pS316-TTP) in serum-shocked mouse NIH 3T3 cells. GAPDH serves as a loading control. (C) Same as panel B, but monitoring TTP in LPS-induced RAW 264.7 mouse macrophage cells.

wild-type TTP and TTP deleted of the CIM. Consistent with previous reports (12, 28), constitutive active MK2 (MK2A) stabilized the TTP target transcript, compared to catalytic dead MK2 (MK2D), although this effect was relatively small (Fig. 6A to D). However, removal of the CIM from TTP, while having only a minor effect on TTP activity in the presence of inactive MK2, dramatically stabilized the target mRNA in the presence of active MK2 (Fig. 6A to D). This stabilization was dependent on the two serines, serines 52 and 178, targeted by MK2 as mutating them to alanines restored the activity of TTP deleted of the CIM in the presence of active MK2 (Fig. 6E to G). Consistent with these observations, treatment of TTP with the phosphatase inhibitor okadaic acid, which causes general upregulation of TTP phosphorylation, caused a reduction in association of TTP with the CCR4-NOT complex as monitored by CNOT1 co-immunoprecipitation, which was exacerbated when the CIM was deleted (Fig. 6H). We observed similar strong dependence on the CIM of TTP activity in the presence of active MK2 when the activity of the $TTP_{PS;WA;\Delta CIM}$ triple mutant was compared to $TTP_{PS;WA}$ (Fig. 7A and B) and when wild-type TTP was compared to TTP mutated at a phenylalanine residue within the CIM important for association with CNOT1 (Fig. 7C and D).

The experiments described above were conducted with tethered TTP. To test whether TTP shows a similar response to MK2 when bound directly to an ARE we repeated the experiments using a β-globin reporter mRNA containing an ARE from the 3'UTR of human GM-CSF mRNA (6). Consistent with observations using the tethered approach, full length TTP promoted efficient decay of the ARE-mRNA even in the presence of active MK2, but its activity in the presence of MK2 was impaired upon deletion of the CIM (Fig. 8A–C).

The TTP-CIM is regulated by phosphorylation independently of MK2. Phosphorylation of the TTP CIM has been previously observed to inhibit association with CNOT1 (8). We therefore wished to test whether CIM phosphorylation regulates TTP activity independently of MK2. We first tested the importance of CIM phosphorylation in

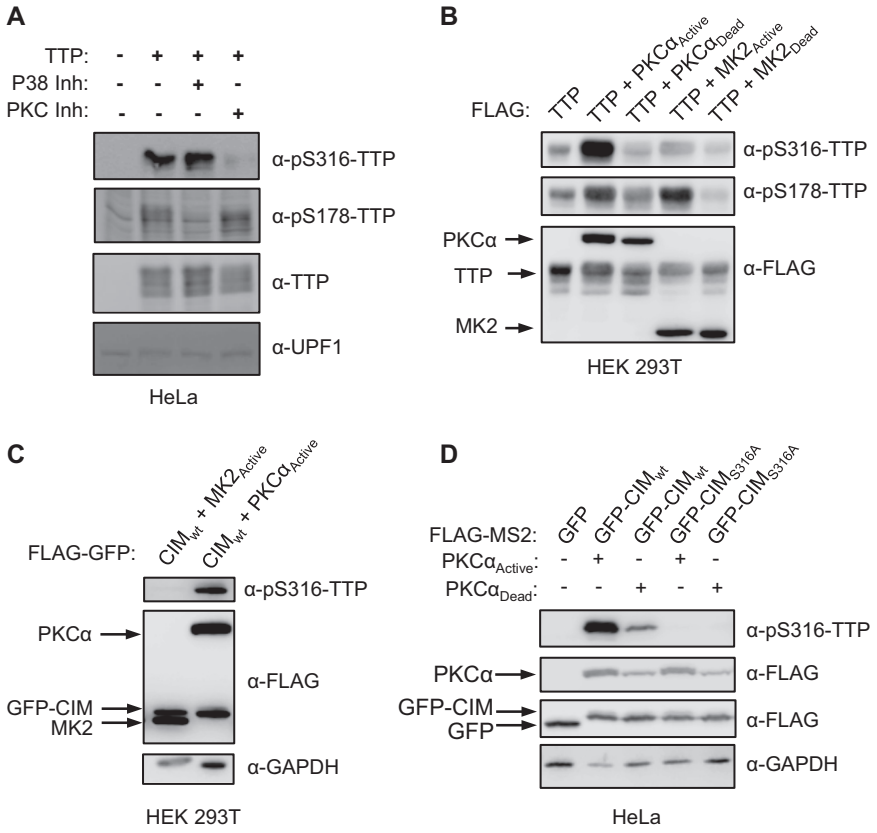

FIG 5 TTP serine 316 is phosphorylated by kinase(s) other than MK2. (A) Western blots monitoring TTP and its phosphorylation at serine 316 (pS316-TTP) or serine 178 (pS178-TTP), exogenously expressed in HeLa cells incubated with inhibitors of p38 (SB203580) or PKC (Gö 6983) kinases. The left lane is a control sample from HeLa cells not expressing TTP. UPF1 served as a loading control. (B) Western blots monitoring phosphorylation of exogenous FLAG-tagged TTP co-expressed with FLAG-tagged, constitutive active or catalytic dead, MK2 or PKCα kinases in HEK293T cells. (C) Western blots monitoring phosphorylation of FLAG-tagged GFP-CIM fusion protein co-expressed with indicated constitutive active kinases in HEK293T cells. (D) Western blots monitoring phosphorylation of FLAG-tagged GFP-CIM and GFP-CIM S316A mutant fusion proteins co-expressed with constitutive active or catalytic dead PKCα kinase in HeLa cells.

the context of full-length TTP. As we observed earlier, TTP is phosphorylated at serine 316 in HeLa Tet-off cells independently of MK2 (Fig. 9A). Mutating serine 316 to an alanine, which prevented phosphorylation of the CIM (Fig. 9A), resulted in a minor increase in the rate of degradation by TTP in the presence of inactive MK2 (Fig. 9B). This effect of the serine 316 to alanine mutation was exacerbated under conditions of active MK2 (Fig. 9B), where TTP activity is increasingly dependent of the CIM (Fig. 6–8). These observations are consistent with the MK2-independent phosphorylation of the CIM inhibiting TTP activity.

To test the importance of the serine 316 residue in mRNA decay activated by the TTP-CIM alone, we mutated this residue to an alanine or a glutamate. MS2-tethered pulse-chase mRNA decay assays showed a minor increase in the degradation rate as a result of the serine to alanine mutation (Fig. 9C and D), and a corresponding minor increase in the rate of deadenylation (Fig. 9E). Expression of PKCα caused an acceleration of mRNA degradation that was independent of TTP-CIM phosphorylation (not shown) and could therefore not be used as a means to test the effect of TTP-CIM phosphorylation. However, mutating serine 316 to a glutamate, which may serve as a phosphomimetic, caused a significant increase in the half-life of the targeted mRNA (Fig. 9F and G). Altogether, these findings demonstrate that the TTP CIM activates mRNA decay in a manner not sensitive to the p38 MAPK-MK2 pathway and suggests that MK2-

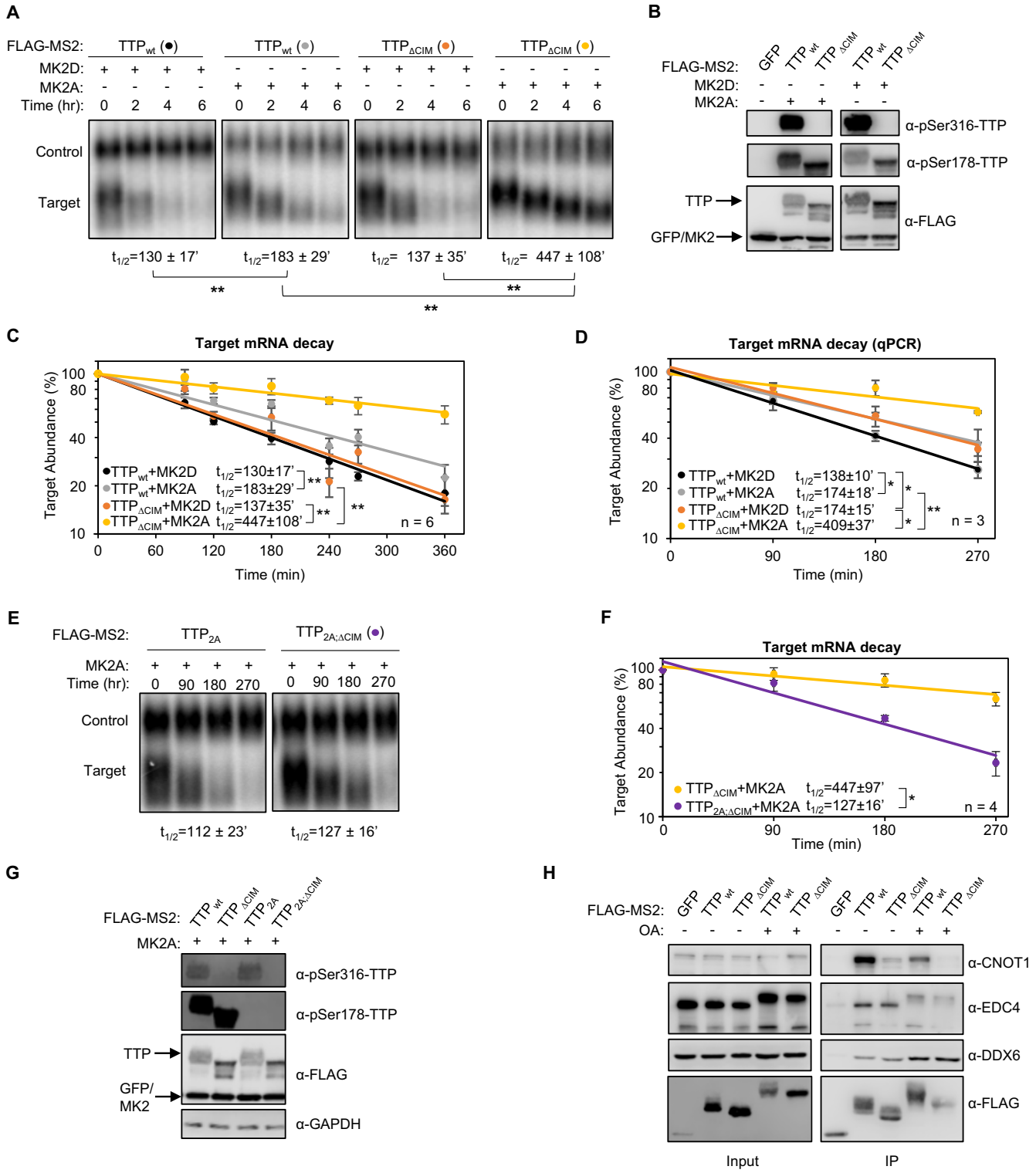

FIG 6 The TTP-CIM remains active in the presence of active MK2. (A) Representative Northern blots monitoring mRNA decay of β-globin mRNA tethered to MS2-TTP wild-type (wt) or ΔCIM proteins, co-expressed with constitutive active (MK2A) or catalytic dead (MK2D) MK2 kinase. (B) Western blots monitoring expression levels of TTP and MK2 proteins in panel A. Note, MS2-GFP and MK2 migrate similarly. (C) Graph quantifying six repeats of mRNA decay assays in panel A. Error bars represent standard deviation. (D) Graph quantifying three repeats of mRNA decay assays as in panel A but quantified by RT-qPCR rather than Northern blotting. (E) Representative Northern blots monitoring mRNA decay of β-globin mRNA tethered to MS2-TTP or MS2-TTP ΔCIM, each with alanine mutations at serines 52 and 178 (2A) and co-expressed with constitutive active MK2 (MK2A). (F) Graph quantifying four repeats of mRNA decay assays monitoring MS2-TTP ΔCIM with and without alanine mutations at serines 52 and 178 (2A) in the presence of active MK2 (MK2A). (G) Western blots monitoring expression levels of TTP and MK2 proteins in panels E and F. (H) Western blot showing proteins co-immunoprecipitating (IP, right panels) with indicated FLAG-tagged TTP proteins expressed in HEK293T cells treated with or without okadaic acid (OA). Input samples corresponding to 2.5% of IPs are shown on the left. *, $p < 0.05$, **, $p < 0.01$; Student's two-tailed *t*-test.

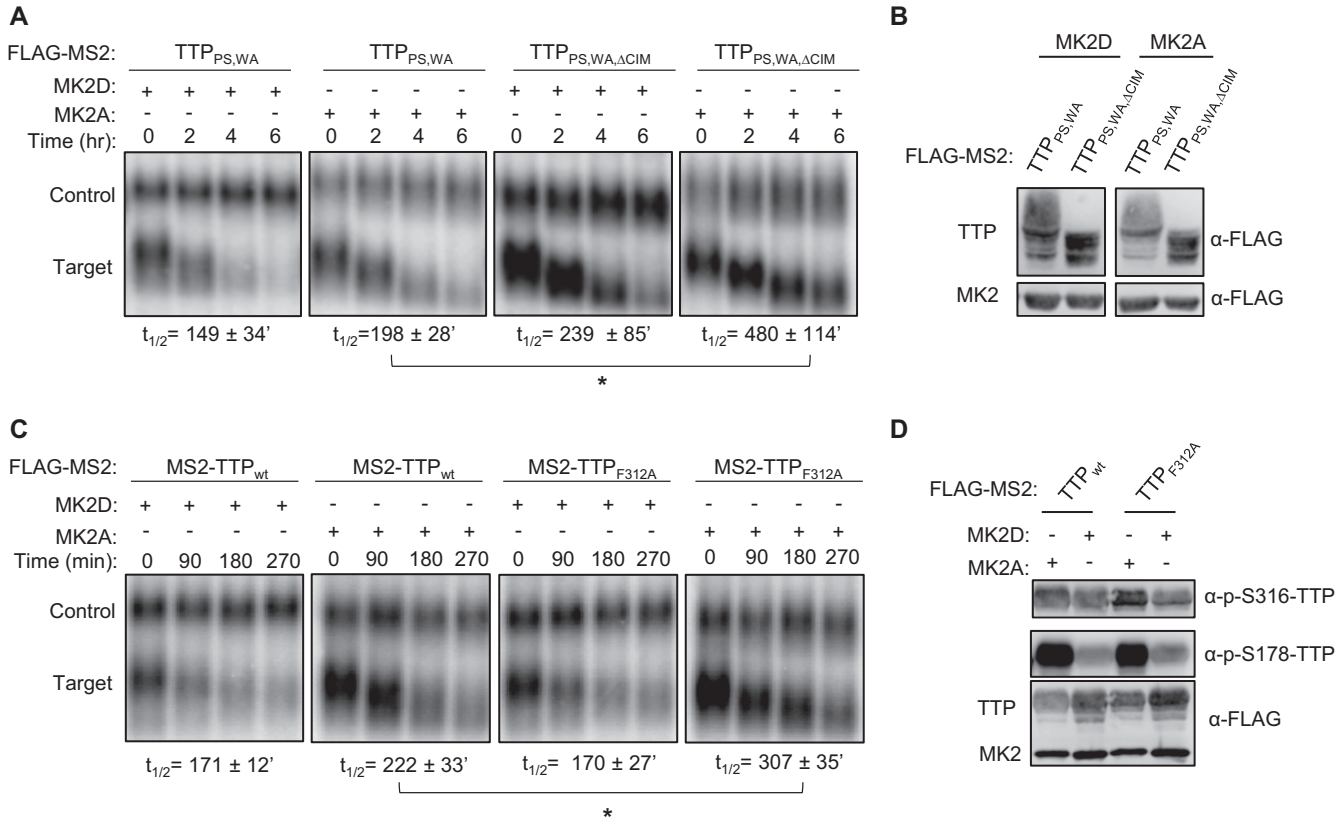

FIG 7 TTP activity is highly dependent on an intact CIM in the presence of MK2. (A, C) Representative Northern blots ($n = 3$) monitoring degradation of β-globin mRNA tethered to indicated MS2-TTP fusion proteins in the presence of constitutive active (MK2A) or catalytically dead (MK2D) MK2 kinase in HeLa tet-off cells. (B, D) Western blots monitoring expression levels of TTP fusion proteins in the experiments in panels A and C, respectively. *, $p < 0.05$; Student's two-tailed *t*-test.

mediated phosphorylation of TTP acts cooperatively with phosphorylation of the CIM by distinct kinase pathway(s) to regulate TTP activity.

DISCUSSION

The regulation of TTP by the p38 MAPK-MK2 pathway during the inflammatory response is a well-established paradigm for the regulation of mRNA decay by signaling. In this study, we demonstrate that the highly conserved C-terminal CIM motif of TTP, which plays a key role in connecting TTP family proteins with the CCR4-NOT deadenylase complex central to mRNA decay, is regulated separately from the p38 MAPK-MK2 pathway. This conclusion is supported by our observations that, unlike TTP serine 178, the TTP CIM serine 316 remained phosphorylated in the presence of a p38 MAPK inhibitor and was not phosphorylated by constitutive active MK2 (Fig. 5). Moreover, TTP remained partially active in the presence of constitutive active MK2, largely due to the activity of the CIM (Fig. 6 to 8). The CIM, in turn, is regulated by other kinases, such as PKCα (Fig. 5), RSK1 (29, 35), and PKA (30), whose phosphorylation of the CIM results in impaired association with CNOT1 of the CCR4-NOT complex and reduced decay activity (8, 31) (Fig. 9). The TTP CIM recruits the CCR4-NOT complex and activates deadenylation and decay in cooperation with conserved tryptophans of TTP (Fig. 1 and 2), which had previously been found to interact with CNOT9 (9). By contrast, disrupting the association of TTP with the 4EHP-GYF2 complex via mutation of TTP tetraproline motifs did not impair TTP-mediated mRNA decay rates (Fig. 3).

Our finding that TTP remains highly active even when deletion of the TTP CIM and mutations in conserved tryptophans and tetraproline motifs disrupt associations with

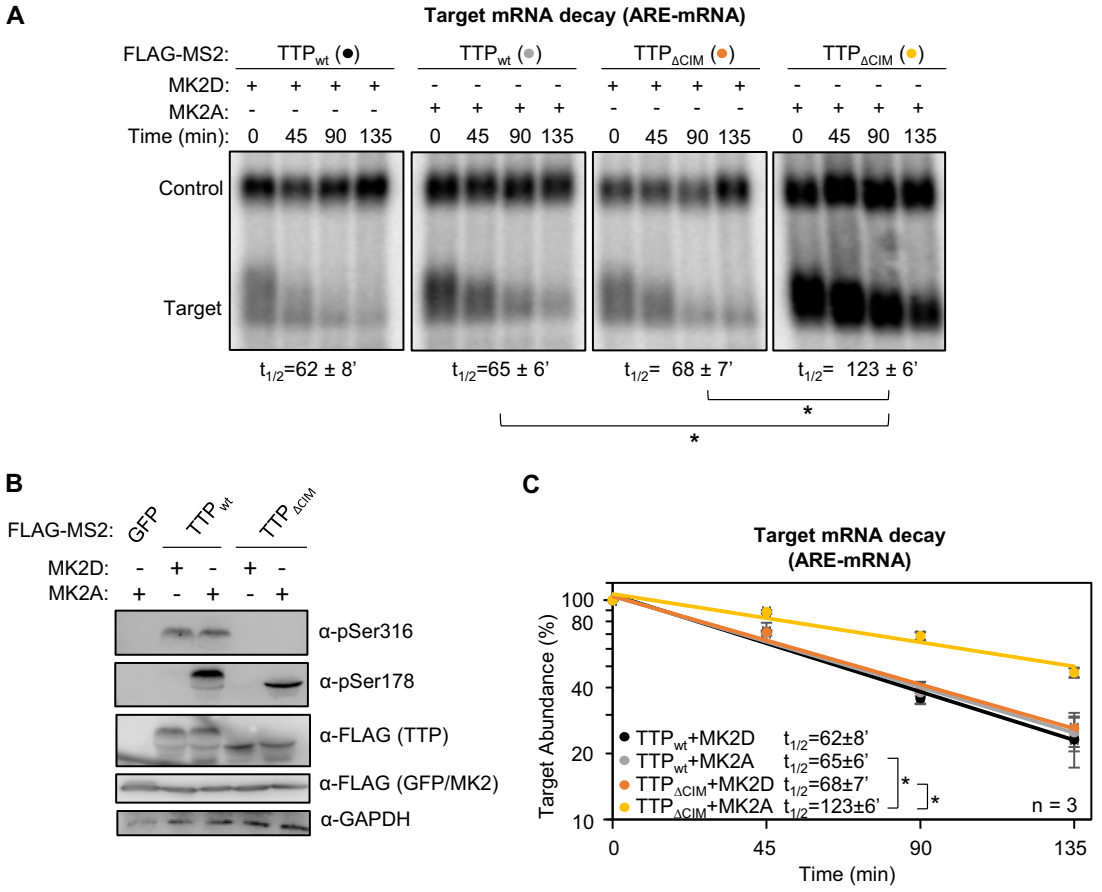

FIG 8 TTP-mediated ARE-mRNA decay is highly dependent of the CIM in the presence of active MK2. (A) Representative Northern blots monitoring mRNA decay of β-globin mRNA containing an ARE from GM-CSF mRNA, in the presence of TTP wild-type (wt) or ΔCIM proteins, co-expressed with constitutive active (MK2A) or catalytic dead (MK2D) MK2 kinase. (B) Western blots monitoring expression levels of TTP and MK2 proteins in panel A. Note, FLAG-MS2-GFP migrates similarly to FLAG-MK2. (C) Graph quantifying three repeats of mRNA decay assays in panel A. Error bars represent standard deviation. *, $p < 0.05$; Student's two-tailed *t*-test.

CCR4-NOT and 4EHP-GYF2 complexes (Fig. 1 and 3), suggests that TTP promotes degradation via additional interactions with cellular RNA decay machinery. This residual activity of TTP may in part be explained by its undisrupted association with decapping factors (Fig. 3). With the exception of its conserved RNA binding zinc-finger domain, TTP is composed of mostly predicted intrinsically disordered regions (23). These types of domains have been implicated in the association with decapping factors and p-bodies and therefore may contribute to the activity of TTP (40–42). It is also possible that additional regions of TTP contribute to the association with the CCR4-NOT complex or other, yet to be determined, mRNA decay factors. Our mutational studies found no rate-limiting role for association with the 4EHP-GYF2 complex in mRNA decay by tethered TTP. 4EHP-GYF2 may specifically promote translation repression (7, 24, 33). The knockout of 4EHP in mouse embryonic fibroblasts caused upregulation of TTP target mRNAs in addition to their encoded proteins (7). This mRNA upregulation could be an indirect effect of interfering with their TTP-mediated translation repression during inflammation. An important goal for future studies will be to identify the complete interaction network of TTP with mRNA decay and translation repression machinery.

The most surprising finding of this study was that the TTP CIM remains active and capable of promoting mRNA decay in the presence of active MK2, despite the p38 MAPK-MK2 pathway having been previously implicated in TTP CIM phosphorylation and inhibition of TTP deadenylase association (28, 29, 31, 34, 43, 44). This observation

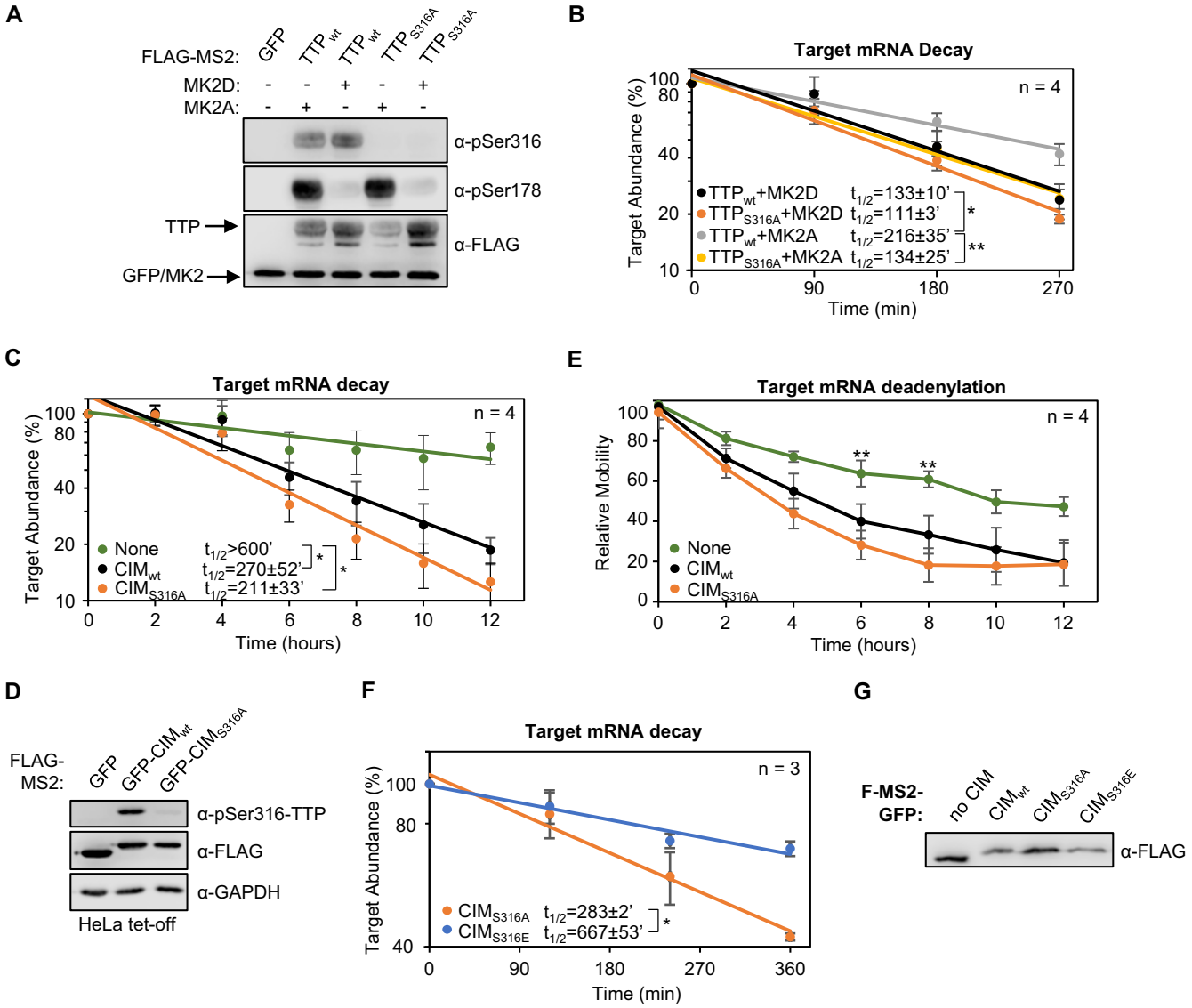

FIG 9 TTP-CIM activity is regulated by phosphorylation independently of MK2. (A) Western blots monitoring phosphorylation of MS2-TTP wild-type (wt) or S316A mutant fusion proteins in the presence of constitutive active (MK2A) or catalytic dead (MK2D) MK2 kinase in HeLa Tet-off cells. (B) Graph quantifying four repeats of mRNA decay assays for β-globin mRNA tethered to MS2-TTP proteins co-expressed with constitutive active (MK2A) or catalytic dead (MK2D) MK2 kinase. Error bars represent standard deviation. (C) Graph quantifying four repeats of mRNA decay assays for β-globin mRNA tethered to indicated MS2-GFP fusion proteins in HeLa Tet-off cells (none: MS2-GFP alone). (D) Western blots monitoring TTP phosphorylation and TTP and MK2 expression levels in panel C. (E) Graph showing relative band mobility as a measure of mRNA deadenylation from the experiments graphed in panel C, measured as described for Fig. 1F Note, the control experiments (*None* and *CIM$_{WT}$*) in panels C-E are identical to the experiments presented in Fig. 1C to F. (F) Graph quantifying three repeats of mRNA decay assays for β-globin mRNA tethered to indicated MS2-GFP-CIM fusion proteins in HeLa Tet-off cells, monitored by RT-qPCR. (G) Western blot monitoring expression levels of fusion proteins in panel F. *, $p < 0.05$, **, $p < 0.01$, Student's two-tailed *t*-test.

suggests that activation of the p38 MAPK-MK2 pathway is insufficient to fully inactivate TTP and cooperativity with one or more additional kinase pathways is required. This has important implications for how TTP activity is repressed in physiological conditions, for example during the inflammatory response when TTP repression allows accumulation of ARE-mRNAs expressing pro-inflammatory cytokines (14–16, 18). The observation that TTP associates with the CCR4-NOT complex via additional interactions beyond the CIM (9) (Fig. 2) may explain how phosphorylation by MK2 of residues outside of the CIM impairs CCR4-NOT association (26, 28–30). The CIM and its phosphorylated serine is a highly conserved motif shared by all members of the ZFP36 family. ZFP36 paralogs have both overlapping as well as unique roles in mRNA decay. Thus, certain kinase pathways may regulate all members of the ZFP36 family, for example via phosphorylation of the

conserved CIM, whereas other kinase pathways may specifically regulate a subset of ZFP36 family members. This may provide specificity to how ARE-mRNA decay is regulated in different cell types and under different conditions.

MATERIALS AND METHODS

Plasmids. pcDNA3-FLAG-MS2 plasmids expressing FLAG-MS2-tagged TTP mutant proteins (Table 1) were generated from previously described pcDNA3-FLAG-MS2-TTP plasmids (28) using site-directed mutagenesis according to the manufacturer's protocol (New England Biolabs). Expression plasmids for FLAG-tagged constitutive active and catalytically dead MK2 kinases were previously described (12, 28). Similarly, expression plasmids for the control β-globin mRNA containing a 3′UTR sequence from GAPDH mRNA and the target tetracycline-regulated β-globin mRNA containing a 3′UTR with six MS2 coat protein stem-loop binding sites were previously described (32). The pcDNA3-FLAG-MS2-GFP-CIM constructs were generated by first generating a pcDNA3-FLAG-MS2-CIM plasmid by inserting the sequence corresponding to mouse TTP residues 304–319 into the pcDNA3-FLAG-MS2 plasmid (6) between restriction sites BamHI and NotI. Gibson Assembly (New England Biolabs, NEB) was subsequently performed to insert the GFP coding region from pSpCas9(BB)-2A-GFP (PX458) into the pcDNA3-FLAG-MS2-CIM vector between the MS2 coat protein and the CIM. pcDNA3-FLAG-PKCα constructs expressing FLAG-tagged PKCα were generated by amplifying the coding region of PKCα from HeLa Tet-off cell total RNA and inserting it into pcDNA3-FLAG (45) immediately downstream of the FLAG peptide sequence using Gibson Assembly (NEB). Constitutive active PKCα-AE was generated by mutating alanine 25 into glutamic acid. Catalytic dead PKCα-KR was generated by mutating lysine 368 into arginine.

Cell culture. HeLa Tet-off, HEK293T, RAW264.7, and NIH3T3 cells were cultured in Dulbecco's modified Eagle's medium (DMEM; Gibco) with 10% fetal bovine serum (FBS) and 1% Penicillin-Streptomycin. For experiments shown in Fig. 4B, NIH3T3 cells were washed with phosphate-buffered saline (PBS) and grown in DMEM containing 0.5% FBS for 24 h. Cells were subsequently treated with DMEM containing 20% FBS for the indicated amount of time and collected in Laemmli sample lysis buffer (2% SDS, 10% Glycerol, 60 mM Tris-HCl pH 6.8, 5% β-mercaptoethanol). For experiments shown in Fig. 4C, RAW264.7 cells were treated with DMEM containing 100 ng/mL lipopolysaccharide (LPS) for the indicated times and collected in sample lysis buffer.

Antibodies. Rabbit polyclonal anti-pS316-TTP antibody was generated with the synthesized oligopeptide PRRLPIFNRI(p)SVSE (Pocono Rabbit Farm & Laboratory, USA). The antiserum was purified by affinity chromatography by first collecting antibody binding to a PRRLPIFNRI(p)SVSE-peptide column, and, after elution, collecting the flow-through from a subsequent unphosphorylated PRRLPIFNRISVSE-peptide column. Immunoblots were probed with the following antibodies at the indicated concentrations: rabbit polyclonal anti-FLAG (Millipore Sigma, F7425; 1:1,000), mouse monoclonal anti-FLAG M2 (Millipore Sigma, F1804; 1:1,000), rabbit polyclonal anti-DDX6 (Bethyl, A300-461A; 1:1,000), rabbit polyclonal anti-GIGYF2 (Santa Cruz Biotechnology, sc-134708; 1:50), mouse monoclonal anti-14-3-3 (Santa Cruz Biotechnology, sc-1657; 1:1,000), rabbit polyclonal anti-TTP (Sigma-Aldrich, T5327; 1:500), rabbit polyclonal anti-CNOT1 (Proteintech, 14276-1-AP; 1:200), rabbit polyclonal anti-CNOT9 (Proteintech, 22503-1-AP, 1:500), mouse monoclonal anti-GAPDH (Cell Signaling Technology, 97166, 1:1,000), rabbit polyclonal anti-EDC4 ((42); 1:200) rabbit polyclonal anti-pSer178-TTP ((11) a generous gift from Dr. Georg Stoecklin, Heidelberg University; 1:500).

Co-immunoprecipitation assays. Co-immunoprecipitation assays were performed as previously described (7). Briefly, confluent HEK 293T cells were split at 1:10 onto 10-cm plates. The following day, samples were transfected with 5 μg of the indicated FLAG-tagged TTP wild-type or mutant expression plasmids using TransIT 293 reagent according to the manufacturer's protocol (Mirus). 48 h after transfection, samples were washed in PBS, pelleted by centrifugation, and collected in hypotonic lysis buffer (10 mM Tris-HCl pH 7.5, 10 mM NaCl, 2 mM EDTA, 0.5% Triton X-100, 1 mM PMSF, 1 μM aprotinin, and 1 μM leupeptin) for 10 min on ice. NaCl concentrations were increased to 150 mM and samples were treated with 50 μg/mL RNase A for 10 min. Samples were centrifuged at 21,130*g* for 15 min at 4°C and supernatants were added to 50 μL of M2 anti-FLAG-agarose beads (Sigma) and nutated for 2 h at 4°C. Beads were washed 4 times with NET-2 (50 mM Tris-HCl pH 7.5, 150 mM NaCl, 0.05% Triton X-100) and resuspended in 50 μL of 2x Laemmli sample lysis buffer (4% SDS, 20% Glycerol, 120 mM Tris-HCl pH 6.8, 10% β-Mercaptoethanol). Samples were separated by SDS-polyacrylamide gel electrophoresis (SDS-PAGE) and analyzed by Western blotting. 0.5% of whole cell extracts and 20% of pull-down elutions were loaded for analyses.

Pulse-chase mRNA decay assays. Tethered mRNA decay assays were performed as previously reported (28, 32). Briefly, confluent HeLa Tet-off cells (TaKaRa Bio) in 10-cm plates were split into 12-well plates at between 1:15 to 1:20. Two days later, cells were transfected with β-globin control (25 ng) and reporter constructs containing MS2 binding sites (250 ng) and FLAG-MS2-TTP constructs (100 ng), or MS2-GFP constructs as a control, using TransIT-HeLaMONSTER transfection kit according to the manufacturer's protocol (Mirus). Cells were subsequently incubated in the presence of 50 ng/mL tetracycline to inhibit expression of the target mRNA. 24 h posttransfection, transcription of the reporter transcripts was pulsed with the addition of fresh media lacking tetracycline for 4–6 h and then treated with 1 μg/mL tetracycline to shut off transcription. Total RNA was harvested at indicated times after transcription shutoff by extraction with TRIzol following the manufacturer's protocol (Thermo Fisher). Samples were analyzed by Northern blotting as previously described (28), or by reverse transcription followed by quantitative PCR (see below). Deadenylated samples were generated by resuspending total RNA in 9 μL water and incubating the samples with 1 μL of 1 mM oligo-dT$_{20}$ at 80°C for 2 min followed by annealing at room temperature

for 5 min. 7 μL of water, 2 μL of 10x RNase H Buffer (500 mM Tris-HCl, 750 mM KCl, 30 mM $MgCl_2$, 100 mM DTT, pH 8.3; NEB) and 1 μL of 5 units/μL RNase H (NEB) were added and samples were incubated at 37°C for 30 min. RNA samples were extracted with phenol:chloroform (1:1), followed by ethanol precipitation, and analyzed by Northern blotting. Half-lives were determined as previously described (32). Briefly, target signal was normalized against control for the corresponding time and plotted on a graph. Slopes of exponential regressions were used to determine the first order decay kinetics to determine mRNA half-lives. Band mobility was determined by plotting signal intensity against migration distance and measuring the mobility of the peak of the target mRNA relative to the peak of the internal control mRNA, with mobility of the target mRNA at the zero-hour time point set to 100 and mobility of the target mRNA after treatment with RNase H and oligo-dT to remove the poly(A)-tail set to 0.

Reverse transcription followed by quantitative PCR (RT-qPCR) assays. Three micrograms of RNA, isolated using TRIzol (Invitrogen) according to the manufacturer's protocol, were incubated with three units of RQ1 RNase-free DNase (Promega) at 37°C for 30 min. RNA was subsequently extracted with phenol:chloroform:isoamyl alcohol (50:49:1), ethanol precipitated, washed with 70% ethanol and dissolved in 10 μL of water (Molecular Biology Grade, IBI Scientific). Two hundred nanograms of DNase-treated RNA was subsequently reverse transcribed using random hexamers with Superscript III reverse transcriptase according to the manufacturer's protocol (Invitrogen). The corresponding cDNA generated was used for qPCR quantification using Fast SYBR green Master Mix (Applied Biosystems) on a StepOnePlus System (Applied Biosystems). qPCR primer-pair efficiency (E) was calculated by plotting $\log_{10}$ dilutions of cDNA versus cycle threshold values. E values greater than 90% were used as a cutoff. The following DNA oligos were used at 200 nM each: For β-globin target mRNA, β-globin_F: CTTCAGGCTCCTGGGCAA and β-globin_Target_R: TGGACAGCAAGAAAGCGA, and for the β-globin Control mRNA: β-globin_F (as above) and β-globin_Control_R: TCTTCTGGGTGGCAGTGATG.

ACKNOWLEDGMENTS

We thank members of the Lykke-Andersen lab, Tim Nicholson-Shaw, Cody Ocheltree, and Tiantai Ma for input on the manuscript. We thank Georg Stoecklin (Heidelberg University) for sharing the anti-p-Ser178-TTP antibody. This work was supported by National Institutes of Health (NIH) fellowship F32 GM128320-03 to A.C. and National Institutes of Health (NIH) grant R35 GM118069 to J. L.-A.

REFERENCES

1. Schoenberg DR, Maquat LE. 2012. Regulation of cytoplasmic mRNA decay. Nat Rev Genet 13:448–448. https://doi.org/10.1038/nrg3254.
2. Garneau NL, Wilusz J, Wilusz CJ. 2007. The highways and byways of mRNA decay. Nat Rev Mol Cell Biol 8:113–126. https://doi.org/10.1038/nrm2104.
3. Hao S, Baltimore D. 2009. The stability of mRNA influences the temporal order of the induction of genes encoding inflammatory molecules. Nat Immunol 10:281–288. https://doi.org/10.1038/ni.1699.
4. Schwanhäusser B, Busse D, Li N, Dittmar G, Schuchhardt J, Wolf J, Chen W, Selbach M. 2011. Global quantification of mammalian gene expression control. Nature 473:337–342. https://doi.org/10.1038/nature10098.
5. Radhakrishnan A, Green R. 2016. Connections Underlying translation and mRNA stability. J Mol Biol 428:3558–3564. https://doi.org/10.1016/j.jmb.2016.05.025.
6. Lykke-Andersen J, Wagner E. 2005. Recruitment and activation of mRNA decay enzymes by two ARE-mediated decay activation domains in the proteins TTP and BRF-1. Genes Dev 19:351–361. https://doi.org/10.1101/gad.1282305.
7. Fu R, Olsen MT, Webb K, Bennett EJ, Lykke-Andersen J. 2016. Recruitment of the 4EHP-GYF2 cap-binding complex to tetraproline motifs of tristetraprolin promotes repression and degradation of mRNAs with AU-rich elements. RNA 22:373–382. https://doi.org/10.1261/rna.054833.115.
8. Fabian MR, Frank F, Rouya C, Siddiqui N, Lai WS, Karetnikov A, Blackshear PJ, Nagar B, Sonenberg N. 2013. Structural basis for the recruitment of the human CCR4-NOT deadenylase complex by tristetraprolin. Nat Struct Mol Biol 20:735–739. https://doi.org/10.1038/nsmb.2572.
9. Bulbrook D, Brazier H, Mahajan P, Kliszczak M, Fedorov O, Marchese FP, Aubareda A, Chalk R, Picaud S, Strain-Damerell C, Filippakopoulos P, Gileadi O, Clark AR, Yue WW, Burgess-Brown NA, Dean JLE. 2018. Tryptophan-mediated interactions between tristetraprolin and the CNOT9 subunit are required for CCR4-NOT deadenylase complex recruitment. J Mol Biol 430:722–736. https://doi.org/10.1016/j.jmb.2017.12.018.
10. Chrestensen CA, Schroeder MJ, Shabanowitz J, Hunt DF, Pelo JW, Worthington MT, Sturgill TW. 2004. MAPKAP kinase 2 phosphorylates tristetraprolin on in vivo sites including Ser178, a site required for 14-3-3 binding. J Biol Chem 279:10176–10184. https://doi.org/10.1074/jbc.M310486200.
11. Sun L, Stoecklin G, Van Way S, Hinkovska-Galcheva V, Guo RF, Anderson P, Shanley TP. 2007. Tristetraprolin (TTP)-14–3-3 complex formation protects TTP from dephosphorylation by protein phosphatase 2a and stabilizes tumor necrosis factor-α mRNA. J Biol Chem 282:3766–3777. https://doi.org/10.1074/jbc.M607347200.
12. Stoecklin G, Stubbs T, Kedersha N, Wax S, Rigby WF, Blackwell TK, Anderson P. 2004. MK2-induced tristetraprolin:14–3-3 complexes prevent stress granule association and ARE-mRNA decay. EMBO J 23:1313–1324. https://doi.org/10.1038/sj.emboj.7600163.
13. Brook M, Tchen CR, Santalucia T, McIlrath J, Arthur JSC, Saklatvala J, Clark AR. 2006. Posttranslational regulation of tristetraprolin subcellular localization and protein stability by p38 mitogen-activated protein kinase and extracellular signal-regulated kinase pathways. Mol Cell Biol 26:2408–2418. https://doi.org/10.1128/MCB.26.6.2408-2418.2006.
14. Carballo E, Gilkeson GS, Blackshear PJ. 1997. Bone marrow transplantation reproduces the tristetraprolin-deficiency syndrome in recombination activating gene-2 (-/-) mice. Evidence that monocyte/macrophage progenitors may be responsible for TNFα overproduction. J Clin Invest 100:986–995. https://doi.org/10.1172/JCI119649.
15. Taylor GA, Carballo E, Lee DM, Lai WS, Thompson MJ, Patel DD, Schenkman DI, Gilkeson GS, Broxmeyer HE, Haynes BF, Blackshear PJ. 1996. A pathogenetic role for TNFa in the syndrome of cachexia, arthritis, and autoimmunity resulting from tristetraprolin (TTP) deficiency. Immunity 4:445–454. https://doi.org/10.1016/s1074-7613(00)80411-2.
16. Carballo E, Lai WS, Blackshear PJ. 1998. Feedback inhibition of macrophage tumor necrosis factor-α production by tristetraprolin. Science 281:1001–1005. https://doi.org/10.1126/science.281.5379.1001.
17. Lai WS, Carballo E, Strum JR, Kennington EA, Phillips RS, Blackshear PJ. 1999. Evidence that tristetraprolin binds to AU-rich elements and promotes the deadenylation and destabilization of tumor necrosis factor alpha mRNA. Mol Cell Biol 19:4311–4323. https://doi.org/10.1128/MCB.19.6.4311.
18. Carballo E, Lai WS, Blackshear PJ. 2000. Evidence that tristetraprolin is a physiological regulator of granulocyte-macrophage colony-stimulating factor messenger RNA deadenylation and stability. Blood 95:1891–1899. https://doi.org/10.1182/blood.V95.6.1891.
19. Blackshear PJ, Perera L. 2014. Phylogenetic distribution and evolution of the linked RNA-binding and NOT1-binding domains in the tristetraprolin

family of tandem CCCH zinc finger proteins. J Interferon Cytokine Res 34:297–306. https://doi.org/10.1089/jir.2013.0150.
20. Maitra S, Chou CF, Luber CA, Lee KY, Mann M, Chen CY. 2008. The AU-rich element mRNA decay-promoting activity of BRF1 is regulated by mitogen-activated protein kinase-activated protein kinase 2. RNA 14:950–959. https://doi.org/10.1261/rna.983708.
21. Otsuka H, Fukao A, Tomohiro T, Adachi S, Suzuki T, Takahashi A, Funakami Y, Natsume T, Yamamoto T, Duncan KE, Fujiwara T. 2020. ARE-binding protein ZFP36L1 interacts with CNOT1 to directly repress translation via a deadenylation-independent mechanism. Biochimie 174:49–56. https://doi.org/10.1016/j.biochi.2020.04.010.
22. Sandler H, Kreth J, Timmers HTM, Stoecklin G. 2011. Not1 mediates recruitment of the deadenylase Caf1 to mRNAs targeted for degradation by tristetraprolin. Nucleic Acids Res 39:4373–4386. https://doi.org/10.1093/nar/gkr011.
23. Lai WS, Stumpo DJ, Wells ML, Gruzdev A, Hicks SN, Nicholson CO, Yang Z, Faccio R, Webster MW, Passmore LA, Blackshear PJ. 2019. Importance of the conserved carboxyl-terminal cnot1 binding domain to tristetraprolin activity in vivo. Mol Cell Biol 39. https://doi.org/10.1128/MCB.00029-19.
24. Tao X, Gao G. 2015. Tristetraprolin recruits eukaryotic initiation factor 4E2 to repress translation of AU-rich element-containing mRNAs. Mol Cell Biol 35:3921–3932. https://doi.org/10.1128/MCB.00845-15.
25. Cuenda A, Rousseau S. 2007. p38 MAP-kinases pathway regulation, function and role in human diseases. Biochim Biophys Acta 1773:1358–1375. https://doi.org/10.1016/j.bbamcr.2007.03.010.
26. Marchese FP, Aubareda A, Tudor C, Saklatvala J, Clark AR, Dean JLE. 2010. MAPKAP kinase 2 blocks tristetraprolin-directed mRNA decay by inhibiting CAF1 deadenylase recruitment. J Biol Chem 285:27590–27600. https://doi.org/10.1074/jbc.M110.136473.
27. Clark AR, Dean JLE. 2016. The control of inflammation via the phosphorylation and dephosphorylation of tristetraprolin: a tale of two phosphatases. Biochem Soc Trans 44:1321–1337. https://doi.org/10.1042/BST20160166.
28. Clement SL, Scheckel C, Stoecklin G, Lykke-Andersen J. 2011. Phosphorylation of tristetraprolin by MK2 impairs AU-rich element mRNA decay by preventing deadenylase recruitment. Mol Cell Biol 31:256–266. https://doi.org/10.1128/MCB.00717-10.
29. Hsieh HH, Chen YA, Chang YJ, Wang HH, Yu YH, Lin SW, Huang YJ, Lin S, Chang CJ. 2021. The functional characterization of phosphorylation of tristetraprolin at C-terminal NOT1-binding domain. J Inflamm 18:1–16. https://doi.org/10.1186/s12950-021-00288-2.
30. Rataj F, Planel S, Desroches-Castan A, Le Douce J, Lamribet K, Denis J, Feige JJ, Cherradi N. 2016. The cAMP pathway regulates mRNA decay through phosphorylation of the RNA-binding protein TIS11b/BRF1. Mol Biol Cell 27:3841–3854. https://doi.org/10.1091/mbc.E16-06-0379.
31. Ronkina N, Shushakova N, Tiedje C, Yakovleva T, Tollenaere MAX, Scott A, Batth TS, Olsen JV, Helmke A, Bekker-Jensen SH, Clark AR, Kotlyarov A, Gaestel M. 2019. The role of TTP phosphorylation in the regulation of inflammatory cytokine production by MK2/3. J Immunol 203:2291–2300. https://doi.org/10.4049/jimmunol.1801221.
32. Clement SL, Lykke-Andersen J. 2008. A tethering approach to study proteins that activate mRNA turnover in human cells. Methods Mol Biol 419:121–133. https://doi.org/10.1007/978-1-59745-033-1_8.
33. Tollenaere MAX, Tiedje C, Rasmussen S, Nielsen JC, Vind AC, Blasius M, Batth TS, Mailand N, Olsen JV, Gaestel M, Bekker-Jensen S. 2019. GIGYF1/2-driven cooperation between ZNF598 and TTP in posttranscriptional regulation of inflammatory signaling. Cell Rep 26:3511–3521.e4. https://doi.org/10.1016/j.celrep.2019.03.006.
34. Tran DDH, Koch A, Saran S, Armbrecht M, Ewald F, Koch M, Wahlicht T, Wirth D, Braun A, Nashan B, Gaestel M, Tamura T. 2016. Extracellular-signal regulated kinase (Erk1/2), mitogen-activated protein kinase-activated protein kinase 2 (MK2) and tristetraprolin (TTP) comprehensively regulate injury-induced immediate early gene (IEG) response in in vitro liver organ culture. Cell Signal 28:438–447. https://doi.org/10.1016/j.cellsig.2016.02.007.
35. Adachi S, Homoto M, Tanaka R, Hioki Y, Murakami H, Suga H, Matsumoto M, Nakayama KI, Hatta T, Iemura SI, Natsume T. 2014. ZFP36L1 and ZFP36L2 control LDLR mRNA stability via the ERK-RSK pathway. Nucleic Acids Res 42:10037–10049. https://doi.org/10.1093/nar/gku652.
36. Xue Y, Liu Z, Gao X, Jin C, Wen L, Yao X, Ren J. 2010. GPS-SNO: Computational prediction of protein s-nitrosylation sites with a modified GPS algorithm. PLoS One 5:e11290-1. https://doi.org/10.1371/journal.pone.0011290.
37. Gschwendt M, Dieterich S, Rennecke J, Kittstein W, Mueller HJ, Johannes FJ. 1996. Inhibition of protein kinase C μ by various inhibitors. Differentiation from protein kinase c isoenzymes. FEBS Lett 392:77–80. https://doi.org/10.1016/0014-5793(96)00785-5.
38. Nakajima K, Tohyama Y, Kohsaka S, Kurihara T. 2004. Protein kinase Cα requirement in the activation of p38 mitogen-activated protein kinase, which is linked to the induction of tumor necrosis factor α in lipopolysaccharide-stimulated microglia. Neurochem Int 44:205–214. https://doi.org/10.1016/S0197-0186(03)00163-3.
39. Pennington K, Chan T, Torres M, Andersen J. 2018. The dynamic and stress-adaptive signaling hub of 14–3-3: emerging mechanisms of regulation and context-dependent protein–protein interactions. Oncogene 37:5587–5604. https://doi.org/10.1038/s41388-018-0348-3.
40. Luo Y, Na Z, Slavoff SA. 2018. P-Bodies: Composition, Properties, and Functions. Biochemistry 57:2424–2431. https://doi.org/10.1021/acs.biochem.7b01162.
41. Franks TM, Lykke-Andersen J. 2007. TTP and BRF proteins nucleate processing body formation to silence mRNAs with AU-rich elements. Genes Dev 21:719–735. https://doi.org/10.1101/gad.1494707.
42. Fenger-Grøn M, Fillman C, Norrild B, Lykke-Andersen J. 2005. Multiple processing body factors and the ARE binding protein TTP activate mRNA decapping. Mol Cell 20:905–915. https://doi.org/10.1016/j.molcel.2005.10.031.
43. Deleault KM, Skinner SJ, Brooks SA. 2008. Tristetraprolin regulates TNF TNF-α mRNA stability via a proteasome dependent mechanism involving the combined action of the ERK and p38 pathways. Mol Immunol 45:13–24. https://doi.org/10.1016/j.molimm.2007.05.017.
44. Schwede A, Ellis L, Luther J, Carrington M, Stoecklin G, Clayton C. 2008. A role for Caf1 in mRNA deadenylation and decay in trypanosomes and human cells. Nucleic Acids Res 36:3374–3388. https://doi.org/10.1093/nar/gkn108.
45. Lykke-Andersen J. 2002. Identification of a human decapping complex associated with hUpf proteins in nonsense-mediated decay. Mol Cell Biol 22:8114–8121. https://doi.org/10.1128/MCB.22.23.8114-8121.2002.